

# Correcting Sky Quality Meter measurements for aging effects using twilight as calibrator

Johannes Puschnig,<sup>1</sup>★ Magnus Näslund,<sup>2</sup> Axel Schwope,<sup>3</sup> Stefan Wallner<sup>4</sup>

<sup>1</sup>Universität Bonn, Argelander-Institut für Astronomie, Auf dem Hügel 71, D-53121 Bonn, Germany

<sup>2</sup>Department of Astronomy, Stockholm University, AlbaNova University Centre, SE-10691 Stockholm, Sweden

<sup>3</sup>Leibniz-Institut für Astrophysik Potsdam (AIP), An der Sternwarte 16, 14482 Potsdam, Germany

<sup>4</sup>Universität Wien, Institut für Astrophysik, Türkenschanzstraße 17, A-1180 Wien, Austria

Submitted to MNRAS, Dec 7, 2020

## ABSTRACT

In the last decade numerous Sky Quality Meters (SQMs) were installed throughout the globe, aiming to assess the temporal change of the night sky brightness (NSB), and thus the change in light pollution. However, it has become clear that SQM readings may be affected by aging effects such as degradation of the sensor sensitivity and/or loss of transmissivity of optical components (filter, housing window). To date, the magnitude of the darkening has not been assessed in a systematic way. We report for the first time on the quantification of the SQM aging effect and describe the applied method. We combine long-term SQM measurements obtained between 2011 and 2019 in Potsdam-Babelsberg (23 km to the southwest of the center of Berlin), Vienna and Stockholm with a readily available empirical twilight model, which serves as calibrator. Twilight SQM observations, calibrated for changing sun altitudes, reveal a linear degradation of the measurement systems (SQM + housing window) with the following slopes:  $34 \pm 4$ ,  $46 \pm 2$  and  $53 \pm 2$  milli-mags<sub>SQM</sub>  $\text{arcsec}^{-2} \text{yr}^{-1}$  for Stockholm, Potsdam-Babelsberg and Vienna. With the highest slope found in Vienna (latitude  $\sim 48^\circ$ ) and the lowest one found in Stockholm (latitude  $\sim 59^\circ$ ), we find an indication for the dependence of the trend on solar irradiance (which is a function of geographic latitude).

**Key words:** light pollution – atmospheric effects – methods: data analysis

## 1 INTRODUCTION

It was shown by numerous studies that the ever increasing amount of *artificial light at night* (ALAN) has far reaching consequences, not only for astronomy, energy consumption and carbon footprint, but also for animal and human health (Chepesiuk 2009; Haim & Portnov 2013; Cho et al. 2015; Garcia-Saenz et al. 2018), ecosystems (Longcore & Rich 2004) and biodiversity (Hölker et al. 2010). Because ALAN impacts life on Earth in such a drastic way, and on a global scale, it was proposed to monitor light pollution in a similar manner as other pollutants. Although no uniform measuring standard has been implemented to date, in recent years, a number of individuals, observatories and organisations have started to monitor the night sky brightness (NSB) using different methods and devices (Hänel et al. 2018), of which the so called *Sky Quality Meter* (SQM), is probably the most widely used one.

SQM networks of larger scale have been established, for example, in Upper Austria<sup>1</sup>, where a total of 23 SQMs are operational since end of 2015 (Posch et al. 2018; Puschnig et al. 2020), with

most of the SQMs mounted at weather stations. Similarly, starting end of 2009, in Galicia (Spain) a number of 20 SQMs were installed at weather stations of the official Galician meteorological agency<sup>2</sup> in cooperation with the University of Santiago de Compostela (Bará et al. 2019). Being part of a meteorological monitoring system makes these two networks to showcases for future monitoring campaigns around the globe. However, other SQM networks of similar scale exist: The Spanish Light Pollution Research collaboration<sup>3</sup> runs 18 devices, the ‘NachtMeetnet’ network (Schmidt & Spoelstra 2020) counts 15 SQMs, the University of Hong Kong<sup>4</sup> owns 19 stations, and seven SQMs are permanently installed in Italy’s Veneto region (Bertolo et al. 2019). Many other small scale networks or single SQMs are found around the globe. Kyba et al. (2015) have compiled many of these heterogeneous data sets and analyzed it in a consistent way to quantify the properties of skylight.

At present, scientific interpretation in terms of long-term trend analysis of the large amount of readily available SQM data, is hindered by the fact that the magnitude of degradation of SQM mea-

★ E-mail: johannes@sonnensystem.at

<sup>1</sup> <https://www.land-oberoesterreich.gv.at/159659.htm>

<sup>2</sup> <http://www.meteogalicia.gal/Caire/brillidoceo.action>

<sup>3</sup> <http://guaix.fis.ucm.es/splpr/SQM-REECL>

<sup>4</sup> <http://nightsky.physics.hku.hk/>

## 2 Puschnig, Näslund, Schwope, Wallner

surements (due to change in sensor sensitivity, filters and/or housing window) on operation timescales of several years is unknown. It is thus a timely matter to understand how SQMs loose the initial calibration when operated over multiple years. In this paper, we quantify the aging effect for the first time, using long-term SQM measurements, re-calibrated during post-processing with twilight models.

## 2 MEASUREMENTS AND DATA

We are operating SQMs in Potsdam-Babelsberg (23 km to the southwest of the center of Berlin), Vienna and Stockholm since 2011, 2012 and 2015 respectively, aiming to monitor light pollution over long time scales. The exact geographical coordinates of the measurement stations are given in Table 1. As the atmospheric composition (aerosols, ozone, particulate matter) plays a major role in interpreting NSB measurements, we further use meteorological parameters obtained through the Copernicus Climate Change Service (C3S) information 2020 and the Copernicus Atmosphere Monitoring Service (CAMS) Information 2020 (Inness et al. 2019), in order to monitor any systematic changes of the atmospheric composition within the period of time under consideration.

### 2.1 SQM measurements

A first analysis of the SQM data obtained in Potsdam-Babelsberg and Vienna was previously presented in (Puschnig et al. 2014b) and (Puschnig et al. 2014a), and some of the Stockholm data was already discussed in (Posch et al. 2018, Section 4.3 therein).

The exact model designation is SQM-LE, indicating that the devices are equipped with a front lens (L) and ethernet (E) connector. The SQMs are permanently installed and point towards the zenith. Given the Gaussian-like angular response as described in Cinzano (2007) the reported radiances in units of  $\text{magSQM arcsec}^{-2}$  are representative for the average zenithal sky brightness found in a circum-zenithal region with a radius of 10 degrees. Our SQMs are controlled via home-brewed Perl scripts, producing measurements at frequencies of approximately 0.14 (IFA, STO) and 0.5 (BA1) Hz. Further technical details are found in Cinzano (2005) and Bará et al. (2019).

### 2.2 Archival Meteorological Data

Large-scale atmospheric and meteorological parameters were obtained through MARS, the Meteorological Archival and Retrieval System, which provides users with meteorological forecast and analysis results from the European Centre for Medium-Range Weather Forecasts (ECMWF) in GRIB format. In particular, we retrieved parameters from ECMWF's re-analysis product 'ERA5' and atmospheric composition (aerosol optical depths, particulate matter) from 'CAMS Near-real-time' data. ERA5 provides data with an hourly validity. However, particulate matter and optical depths, are

**Table 1.** Locations, station codes, device serial numbers (SN) and geographical coordinates (lat, lon) of the SQMs

Country, City, District	Code	SN	Lat	Lon
SE, Stockholm, Östermalm	STO	2785	59°21'12"N	18°3'28"E
DE, Potsdam, Babelsberg	BA1	–	52°22'48"N	13°6'22"E
AT, Vienna, Währing	IFA	1898	48°13'54"N	16°20'3"E

available only through forecast models with a validity given in 3-hour steps. The spatial resolution of the data grid is 30 and 80km for ERA5 and CAMS Near-real-time respectively. Furthermore, some parameters (e.g. particulate matter) are only available starting from 2015. Relevant parameters for the three cities of Vienna, Potsdam and Stockholm are shown in Figures A1–A3.

## 3 MODELS AND METHODS

In order to reveal the existence of darkening of SQM measurements over time, we use empirical twilight models previously published by Patat et al. (2006) as calibration source. In particular, the temporal change of the difference between predicted NSB (mdl) and the observed one (obs),  $\Delta_{\text{mdl-obs}}$ , will be used as a proxy of the aging effect. The models are based on a statistically significant sample of thousands of *UBVRI* (Johnson-Cousins system) twilight sky flats obtained during several years on mount Paranal (Chile) as part of an instrument calibration procedure. Hence, they are valid only for a limited range of solar zenith distances ( $z$ ), i.e. 95–105°. The functional (polynomial) form for the zenithal NSB during twilight is shown in equation 1. The coefficients for the *BVR* filters are found in Table 2.

$$NSB = a_0 + a_1 * (z - 95) + a_2 * (z - 95)^2 \quad (1)$$

Given the fact that the calculation of atmospheric diffuse flux is a rather complicated problem that requires a detailed treatment of multiple scatterings (Kocifaj & Bará 2019) and knowledge of atmospheric composition such as aerosols, ozone and particulate matter (Joseph et al. 1991; Ścieżor & Kubala 2014; Ścieżor & Czaplicka 2020), it is expected that the residuals of  $\Delta_{\text{mdl-obs}}$  show discrepancies. However, the *average* magnitude of these discrepancies should be independent of time, as long as the *average* atmospheric composition has not changed significantly. In that case, and as long as a large number of independent observations were carried out, one would expect that the residual of  $\Delta_{\text{mdl-obs}}$ , measured over multiple years, is given by a constant, plus scatter with a roughly constant magnitude, caused by complex atmospheric physics. We may thus formulate the null hypothesis that any temporal trend (slope) in the residual (twilight model minus SQM measurements) is caused by instrumental effects (i.e. the SQM aging effect), as long as the *average* composition of the atmosphere has not changed significantly (towards lower abundances) within the same period of time. We would further expect that the degree of darkening (aging effect) is a function of solar surface radiance. Given the range in geographic latitudes of our measurement stations it is thus expected that the effect of darkening is weakest in Stockholm and strongest in Vienna.

In addition to the previously described scatter of  $\Delta_{\text{mdl-obs}}$ , clouds have a strong impact on NSB (Puschnig et al. 2014b; Jechow et al. 2017, 2019). We thus aim to select only clear-sky twilight measurements. To do so, we slice our observations into 5-minute data chunks and evaluate the standard deviation after subtraction of a linear fit. The latter is used as a proxy for cloud coverage. Note that it was previously shown by Cavazzani et al. (2020) that the standard

**Table 2.** Coefficients of the empirical polynomial twilight model of Patat et al. (2006) for the Johnson-Cousins *B*, *V* and *R* filter.

filter	$a_0$	$a_1$	$a_2$
B	11.84	1.411	-0.041
V	11.84	1.518	-0.057
R	11.40	1.567	-0.064

deviation of SQM measurements may serve as clear sky indicator. For the clear-sky case, the following assumptions are made: the maximum deviation is lower than  $0.06 \text{ mag}_{\text{SQM}} \text{ arcsec}^{-2}$  and the standard deviation is lower than  $0.02 * \sqrt{\text{sampling}_{\text{nominal}} / \text{sampling}}$ , with the nominal sampling frequency being 0.14 Hz (IFA, STO). In order to avoid any influence ALAN might have, we only consider twilight observations with sun altitudes between  $-6$  and  $-7^\circ$ , i.e. the bright end of the models with NSBs of approximately  $13$ – $14.5 \text{ mag}_{\text{SQM}} \text{ arcsec}^{-2}$ . Given typical clear-sky NSBs between  $18$ – $20 \text{ mag}_{\text{SQM}} \text{ arcsec}^{-2}$  observed in the three cities, our twilight measurements fall within brightness levels that are at least a factor of 25 higher than those used for the assessment of light pollution. Any contribution of ALAN to our measurements is thus negligible. Analogue, we consider only data with moon altitudes lower than  $-5^\circ$ . The final set of data points ( $\Delta_{\text{mdl-obs}}$ ) are thus the 5-minute averages of the difference between the model and the SQM observations, under clear sky.

## 4 RESULTS

A qualitative comparison between the twilight models as described in Section 3 and two selected scotographs obtained on April 12, 2012 in Vienna and on June 30, 2019 in Stockholm, demonstrates that the polynomial models are indeed an eligible approximation for the true decline of zenithal NSB as observed with the SQM (see Figure 1), at least as long as ALAN’s contribution to NSB is negligible. The figure also shows that the functional form of the modeled gradual decline is very similar in all three filters, in particular in the regime of interest for this work, i.e. when the sun is found between  $-6$  and  $-7^\circ$ . However, the absolute difference between models and data is smallest in ( $B - \text{SQM}$ ). Therefore, we decided to use the  $B$ -band models as a reference. The top panel in Figure 1 further reveals that, in Vienna under clear sky, light pollution starts to dominate the observed NSB once the Sun has declined more than approximately 10 degrees below the horizon. Note that at this point the observed brightness levels are already  $2.5$ – $3.5 \text{ mag}_{\text{SQM}} \text{ arcsec}^{-2}$  higher (darker) than during the range that is used for the calibration of the SQM measurements during post-processing.

Resembling previous results of Puschnig et al. (2014b), the overall level of light pollution (deduced from zenithal NSB) is much lower for the SQM station in Potsdam. The scotograph in the top panel of Figure 2 demonstrates that ALAN starts to dominate from sun altitudes of approximately  $-12$  degrees only. When browsing through the available scotographs<sup>5</sup>, one may already qualitatively assess the effect of darkening, in particular for the 9-year long data series of Potsdam (see Figure 2). We stress that this is only a showcase-comparison, because the atmospheric composition has a strong impact on NSB. And given the fact that the atmospheric composition may change on a daily and seasonal basis, it is expected that the aging effect itself is buried in a large scatter. However, the null hypothesis is that the average of  $\Delta_{\text{mdl-obs}}$  should remain constant over multiple years, as long as the atmospheric composition did not systematically change. On the other hand, any time-dependent trend of  $\Delta_{\text{mdl-obs}}$  must then be caused by instrumental effects, i.e. instrumental aging of the device due to permanent exposure to solar irradiance. After filtering and slicing our SQM measurements into clear-sky chunks with a length of 5 minutes as explained in Section

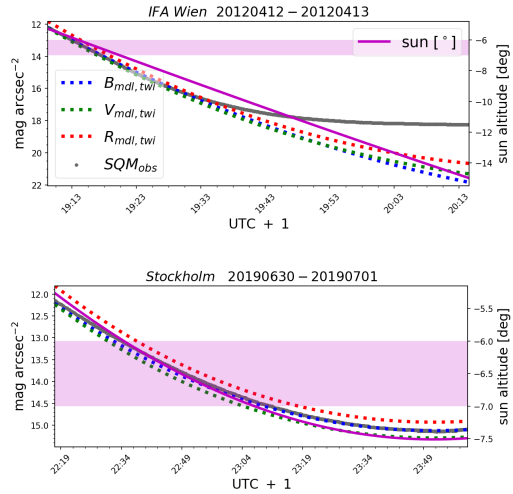


**Figure 1.** Exemplary scotographs of SQM measurements (gray curve) obtained during the course of dusk under clear sky in Vienna on April 12, 2012 (top panel) and in Stockholm on June 30, 2019 (bottom panel). Twilight BVR models are shown in blue, green and red respectively. The magenta solid curve indicates the solar altitude and the highlighted area is the sun altitudes interval  $[-6^\circ, -7^\circ]$  that was used for calibration.

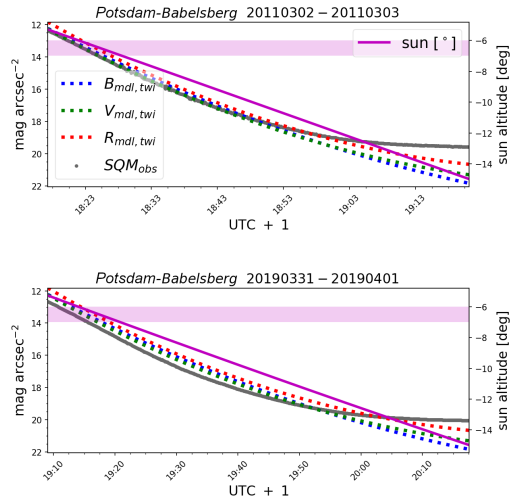


**Figure 2.** Scotographs of SQM measurements (gray curve) obtained during the course of dusk under clear sky in Potsdam on March 2, 2011 (top panel) and March 31, 2019 (bottom panel). The comparison qualitatively shows the darkening effect after 9 years of operation. For more details, see caption of Figure 1.

3, a relatively strong trend (see Figures 3–5) is revealed, suggesting that the SQM measurements are indeed affected by average darkening levels of  $34 \pm 4$ ,  $46 \pm 2$  and  $53 \pm 2 \text{ milli-} \text{mag}_{\text{SQM}} \text{ arcsec}^{-2} \text{ yr}^{-1}$  for Stockholm, Potsdam-Babelsberg and Vienna. Note that the linear regressions in Figures 3–5 were derived under usage of weights, with the latter given by the variance of the data within the 5 minute long chunks. The fitting results are presented in Table 3. We stress that the shape of the probability density distributions of NSB values in the right panels of Figures 3–5 are indicative for the successful removal of data affected by clouds. Because in the latter case, one would expect an asymmetric distribution (log-normal with negative skewness) of NSB values (compare Ścieżor 2020).

<sup>5</sup> All data is available for download and examination via <https://astro.univie.ac.at/en/about-us/light-pollution/>

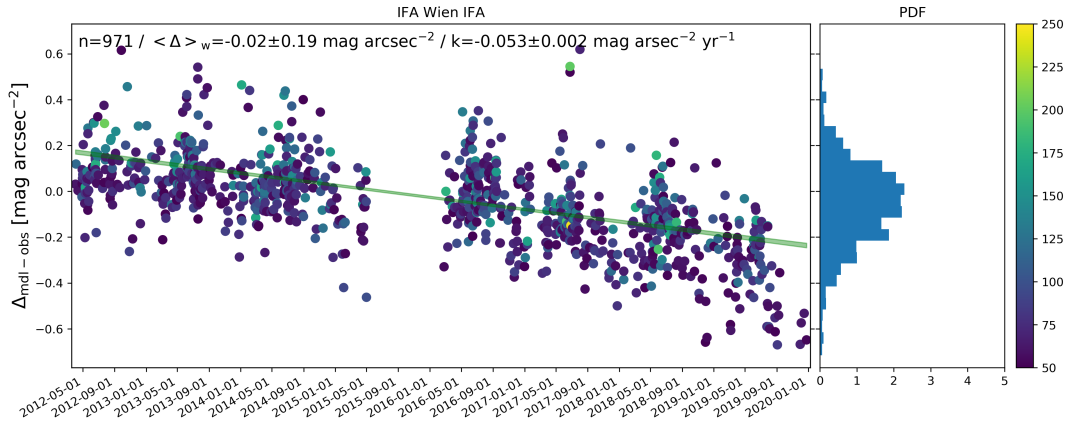


**Figure 3.** SQM aging function for Vienna (latitude  $\sim 48^\circ$ ), derived from calibrating SQM measurements (obtained between 2012 and 2019) with twilight models. Time (x-axis) vs. difference of modeled *B*-filter radiance minus observed SQM radiance (y-axis). Each point is the 5-minute average value obtained under *clear sky* and within a narrow interval of sun altitudes  $[-6^\circ, -7^\circ]$ . The color represents the inverse variance of the underlying SQM data (5-minute time intervals). For example, a value higher than 100 means that the standard deviation (of the model-observation difference) within the time interval was lower than  $0.1 \text{ mag}_{\text{SQM}} \text{ arcsec}^{-2}$ . The green shaded region is the result from a weighted linear fit through the data including the  $\pm 1$ -sigma error range, using the inverse variance as weights.

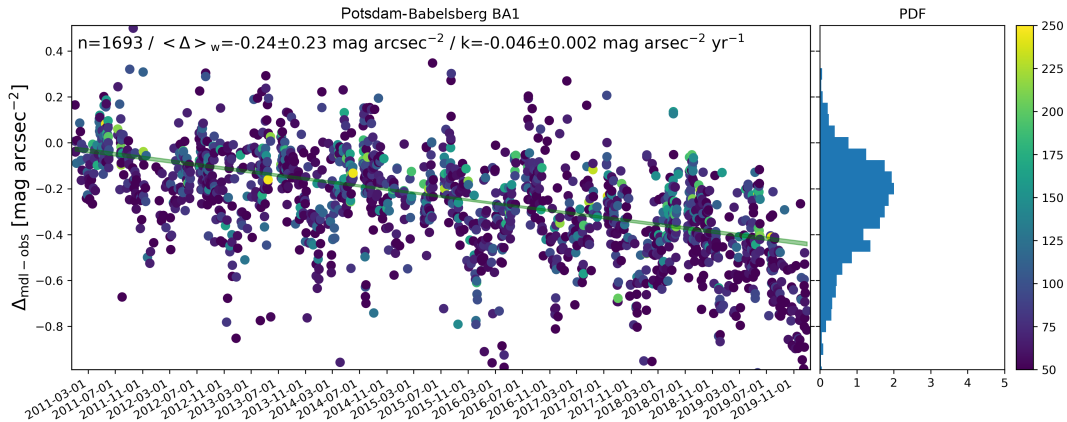


**Figure 4.** SQM aging function for Potsdam (latitude  $\sim 52^\circ$ ), derived from calibrating SQM measurements (obtained between 2011 and 2019) with twilight models. See caption of Figure 3 for more details.

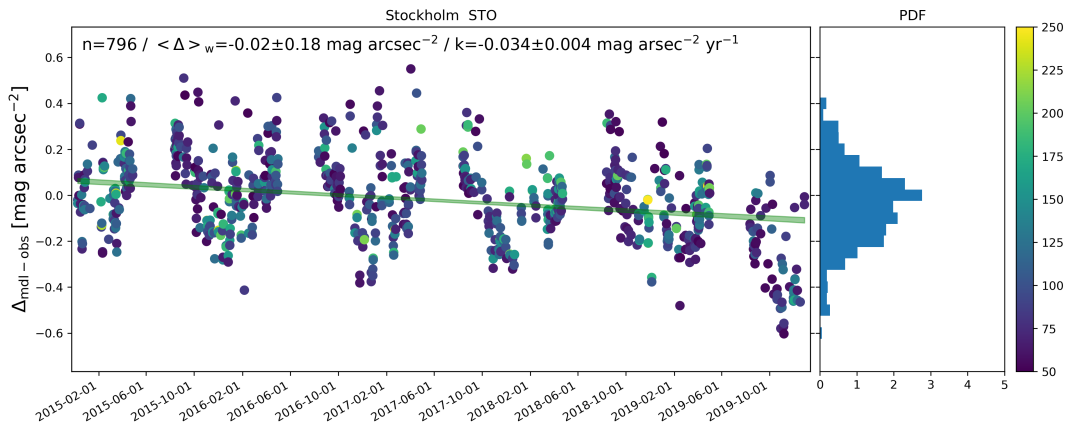


**Figure 5.** SQM aging function for Stockholm (latitude  $\sim 59^\circ$ ), derived from calibrating SQM measurements (obtained between 2015 and 2019) with twilight models. See caption of Figure 3 for more details.

**Table 3.** SQM aging functions from weighted linear regression

station code	slope [magsQM arcsec <sup>-2</sup> yr <sup>-1</sup> ]	intercept [magsQM arcsec <sup>-2</sup> ]
STO	-0.034 ± 0.004	68 ± 8
BA1	-0.046 ± 0.002	92 ± 3
IFA	-0.053 ± 0.002	106 ± 4

## 5 DISCUSSION

Beside the aging trend, Figures 3–5 show strong seasonal NSB variations, in particular for Stockholm. It seems that the amplitude of the seasonal variation is a function of geographic latitude as well. A possible explanation for that may be the increase of snow coverage and snow depth with latitude, leading to stronger variations in surface albedo, that in turn have strong impact on the NSB measurements (compare Wallner & Kocifaj 2019).

The Stockholm data also show another peculiarity, i.e. gaps in data during summer. The reason is the stringent filtering for clear-skies using an upper limit standard deviation (after subtraction of a linear fit from the SQM data) within 5-minute intervals. In Stockholm, for few days around summer solstice, the Sun’s rate of decline per unit time is far from being constant (within the interval of interest). In this case, the polynomials of the Patat et al. (2006) twilight models appear to systematically differ from the observations.

Finally, it is seen in Figures 3–5 that *individual measurements* obtained under clear sky may differ by a large amount, even up to 1 magsQM arcsec<sup>-2</sup> (or a factor of 2.5) on timescales of days or weeks. This scatter is mainly caused by complex atmospheric physics (e.g. short-term changes of atmospheric composition). It is thus important having obtained a statistically significant number of measurements in order to perform an unbiased long-term trend study.

## 6 SUMMARY AND CONCLUSION

Aiming to study the darkening of SQM measurements with time, we have compared readily available twilight models (Patat et al. 2006) with long-term (5–9 years) zenithal NSB measurements obtained during twilight with SQMs at three different sites (Vienna, Potsdam-Babelsberg and Stockholm). Using only measurements obtained at solar zenith angles between 96 and 97°, allows us to focus on brightness levels in which ALAN’s contribution to the zenithal NSB is negligible (likely true for most sites on Earth). Further slicing and filtering the data into clear-sky chunks (using the standard deviation as a clear sky indicator), reveals not only strong seasonal variations, but also an instrumental darkening effect that is well described by a linear fit with slopes of 34±4, 46±2 and 53±2 millimagsQM arcsec<sup>-2</sup> yr<sup>-1</sup> for Stockholm, Potsdam-Babelsberg and Vienna (see Figures 3–5). Given the strong influence of atmospheric composition on NSB, we have checked large-scale atmospheric parameters (AOD, particulate matter, ozone) for existing trends that might cause the observed darkening. As shown in Figures A1–A3 no significant trend was found that could possibly lead to the observed slopes. However, we do notice a slight upward trend of particulate matter, apparent at all three sites. This might have some impact on the derived slopes, due to an increased fraction of (back-)scattering of light, and would even increase the observed aging slopes.

## ACKNOWLEDGEMENTS

Part of this work has been generated using Copernicus Climate Change Service information 2020 and Copernicus Atmosphere Monitoring Service Information 2020.

## REFERENCES

Bará S., Lima R. C., Zamorano J., 2019, *Sustainability*, 11

Bertolo A., Binotto R., Ortolani S., Sapienza S., 2019, *Journal of Imaging*, 5

Cavazzani S., Ortolani S., Bertolo A., Binotto R., Fiorentin P., Carraro G., Saviane I., Zitelli V., 2020, *MNRAS*, 493, 2463

Chepesiuk R., 2009, *Environmental health perspectives*, 117, A20

Cho Y., Ryu S.-H., Lee B., Kim K., Lee E., Choi J., 2015, *Chronobiology international*, 32, 1

Cinzano P., 2005, Technical report, Night Sky Photometry with Sky Quality Meter, <http://www.inquinamentoluminoso.it/download/sqmreport.pdf>. Dipartimento di Astronomia, Vicoletto dell’Osservatorio 2, I-35100 Padova, Italy, Istituto di Scienza e Tecnologia dell’Inquinamento Luminoso, Via Roma 13, I-36106 Thiene, Italy, <http://www.inquinamentoluminoso.it/download/sqmreport.pdf>

Cinzano P., 2007, Technical report, Report on Sky Quality Meter, version L, <http://unihedron.com/projects/sqm-1/sqmreport2.pdf>. Dipartimento di Astronomia, Vicoletto dell’Osservatorio 2, I-35100 Padova, Italy, Istituto di Scienza e Tecnologia dell’Inquinamento Luminoso, Via Roma 13, I-36106 Thiene, Italy, <http://unihedron.com/projects/sqm-1/sqmreport2.pdf>

Garcia-Saenz A., et al., 2018, *Environmental Health Perspectives*, 126, 047011

Haim A., Portnov B. A., 2013, *Light Pollution as a New Risk Factor for Human Breast and Prostate Cancers*, 1st ed. 2013. edn. Springer Netherlands

Hölker F., Wolter C., Perkin E., 2010, *Trends in ecology & evolution*, 25, 681

Hänel A., et al., 2018, *Journal of Quantitative Spectroscopy and Radiative Transfer*, 205, 278

Inness A., et al., 2019, *Atmospheric Chemistry and Physics*, 19, 3515

Jechow A., Kolláth Z., Ribas S. J., Spoelstra H., Hölker F., Kyba C. C. M., 2017, *Scientific Reports*, 7, 6741

Jechow A., Hölker F., Kyba C. C. M., 2019, *Scientific Reports*, 9, 1391

Joseph J. H., Kaufman Y. J., Mekler Y., 1991, *Appl. Opt.*, 30, 3047

Kocifaj M., Bará S., 2019, *Monthly Notices of the Royal Astronomical Society*, 490, 1953

Kyba C. C. M., et al., 2015, *Scientific Reports*, 5

Longcore T., Rich C., 2004, *Frontiers in Ecology and the Environment*, 2, 191

Patat F., Ugnolnikov O. S., Postylyakov O. V., 2006, *A&A*, 455, 385

Posch T., Binder F., Puschnig J., 2018, *J. Quant. Spectrosc. Radiative Transfer*, 211, 144

Puschnig J., Posch T., Uttenhahler S., 2014a, *J. Quant. Spectrosc. Radiative Transfer*, 139, 64

Puschnig J., Schwope A., Posch T., Schwarz R., 2014b, *J. Quant. Spectrosc. Radiative Transfer*, 139, 76

Puschnig J., Wallner S., Posch T., 2020, *MNRAS*, 492, 2622

Schmidt W., Spoelstra H., 2020, Darkness monitoring in the Netherlands 2009–2019, doi:10.5281/zenodo.4293366, <https://doi.org/10.5281/zenodo.4293366>

Wallner S., Kocifaj M., 2019, *J. Quant. Spectrosc. Radiative Transfer*, 239, 106648

Ściążor T., 2020, *Journal of Quantitative Spectroscopy and Radiative Transfer*, 247, 106962

Ściążor T., Czaplicka A., 2020, *Journal of Quantitative Spectroscopy and Radiative Transfer*, 254, 107168

Ściążor T., Kubala M., 2014, *Monthly Notices of the Royal Astronomical Society*, 444, 2487

**APPENDIX A: ADDITIONAL TABLES AND FIGURES**

See next page.

This paper has been typeset from a  $\text{\TeX}$ / $\text{\LaTeX}$  file prepared by the author.

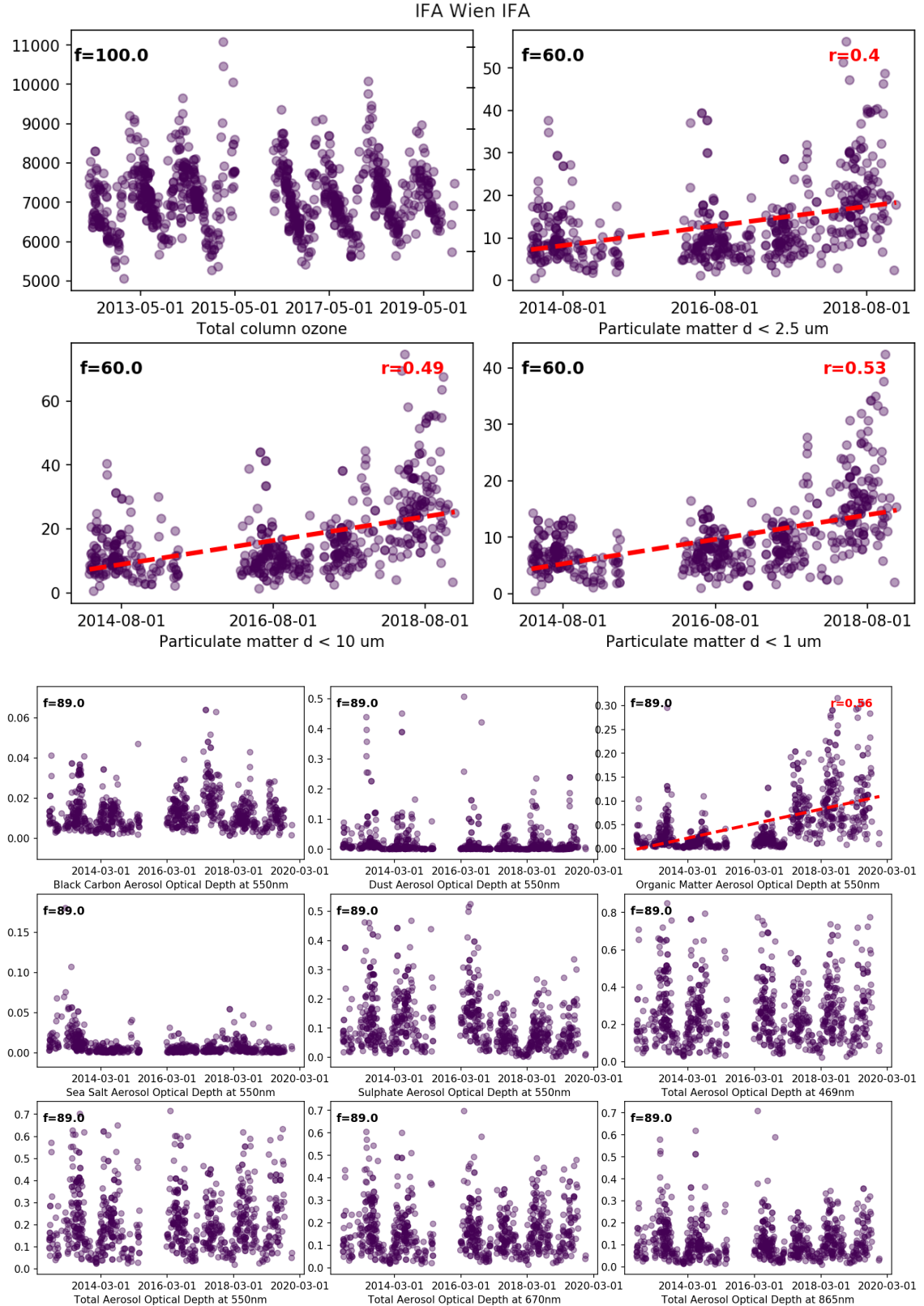


**Figure A1.** Large-scale particulate matter (*top panel*) and aerosol optical depth (*bottom panel*) development for Vienna. The parameter ‘f’ in the top left corner indicates what fraction of available SQM measurements could be matched with the meteorological data shown here. The y-axes units are nm for molecular columns and  $\text{g cm}^{-3}$  for particulate matter.

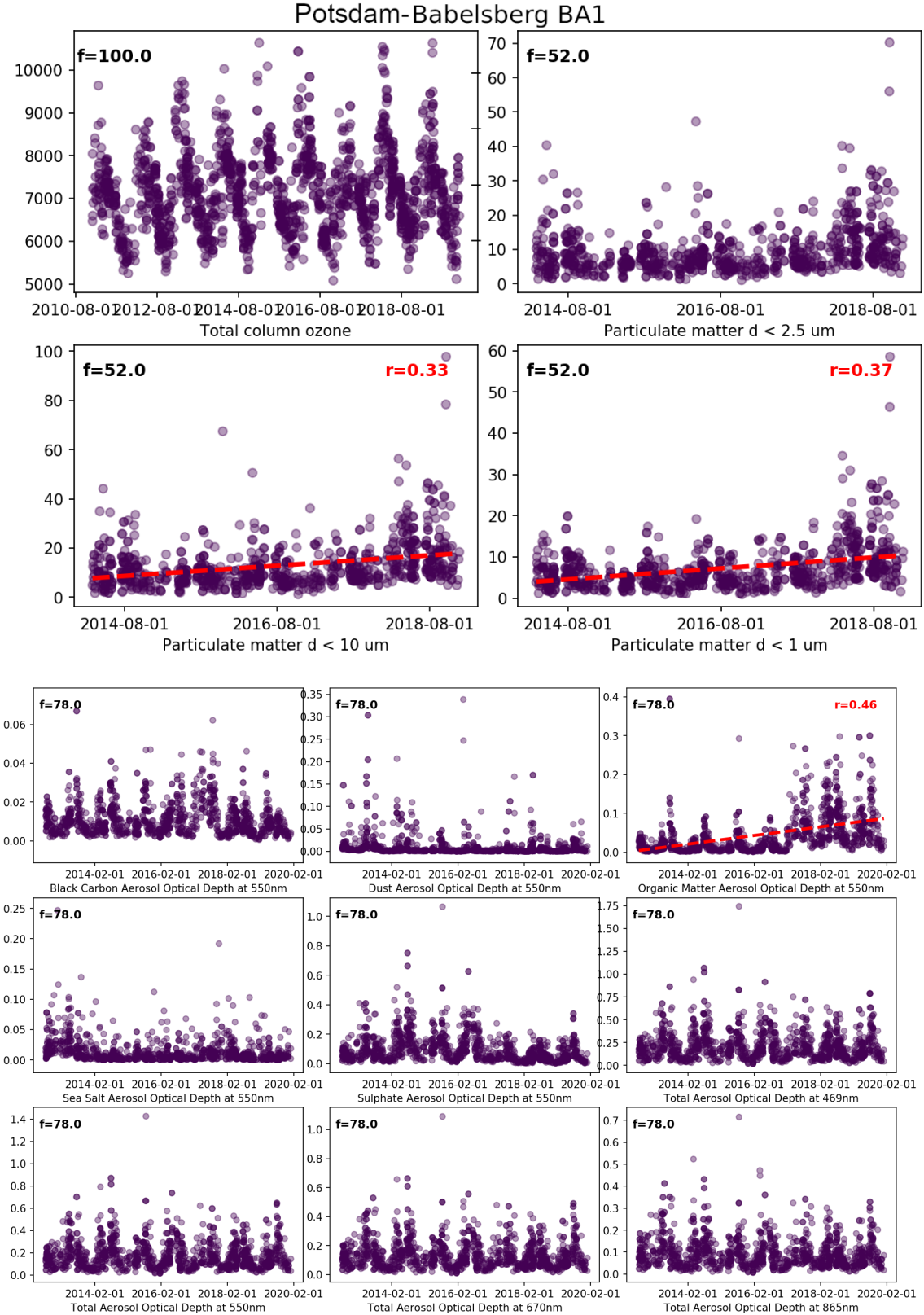


**Figure A2.** Large-scale particulate matter (*top panel*) and aerosol optical depth (*bottom panel*) development for Potsdam. The parameter ‘ $f$ ’ in the top left corner indicates what fraction of available SQM measurements could be matched with the meteorological data shown here. The y-axes units are nm for molecular columns and  $g \text{ cm}^{-3}$  for particulate matter.

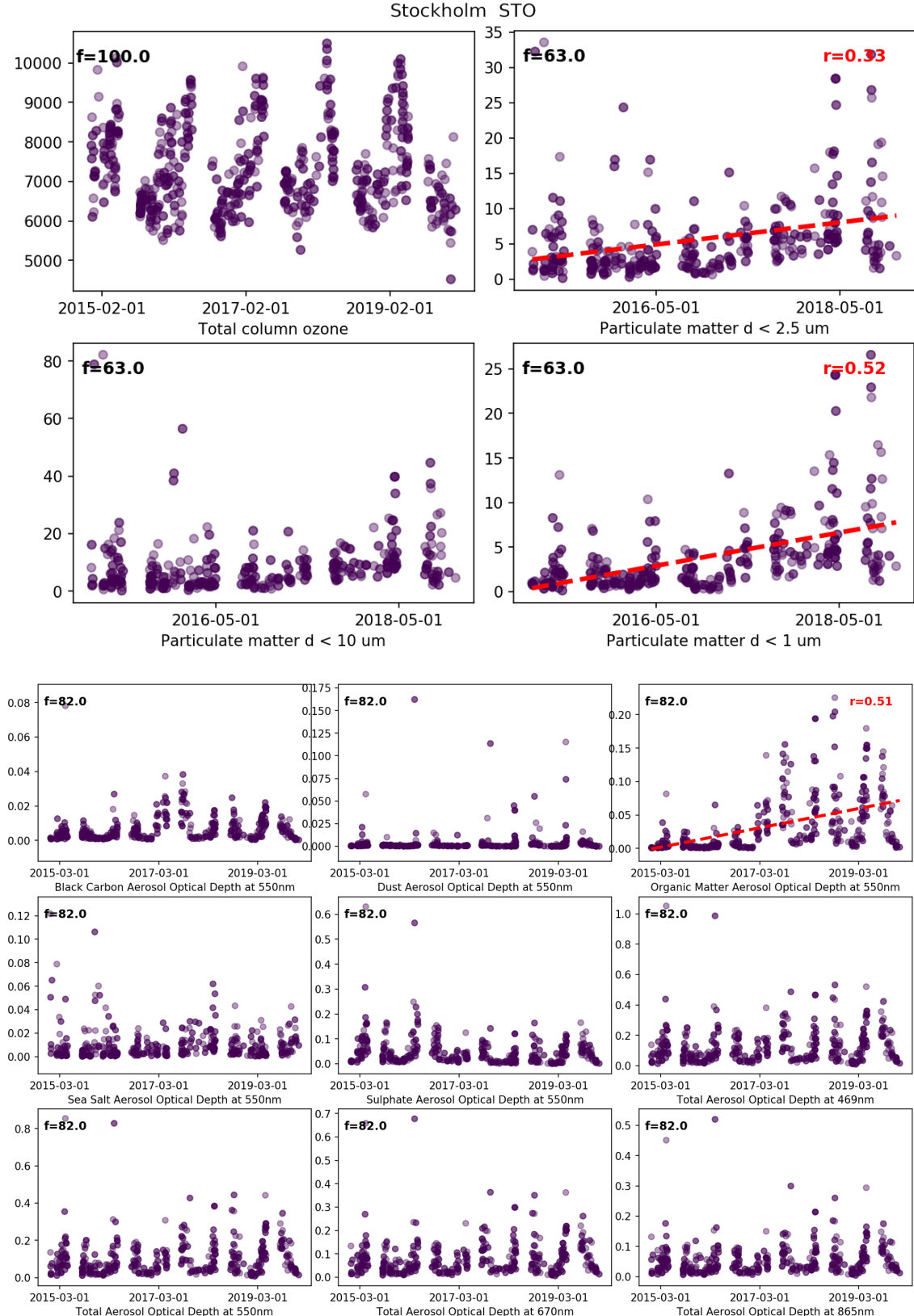


**Figure A3.** Large-scale particulate matter (*top panel*) and aerosol optical depth (*bottom panel*) development for Stockholm. The parameter ‘ $f$ ’ in the top left corner indicates what fraction of available SQM measurements could be matched with the meteorological data shown here. The y-axes units are  $\text{nm}$  for molecular columns and  $\text{g cm}^{-3}$  for particulate matter.